Combining Monte Carlo generators with next-to-next-to-leading order calculations: event reweighting for Higgs boson production at the LHC

Giovanna Davatz[a], Fabian Stöckli[a], Charalampos Anastasiou[a], Günther Dissertori[a], Michael Dittmar[a], Kirill Melnikov[b], Frank Petriello[c]

[a]*Institute of Particle Physics, ETH, 8093 Zurich, Switzerland*
[b]*Department of Physics and Astronomy, University of Hawaii,*
2505 Correa Rd., Honolulu, Hawaii 96822
[c]*University of Wisconsin, Madison, WI 53706,*
USA and Fermi National Accelerator Laboratory,
P.O. Box 500, MS 106, Batavia, IL 60510, USA

Abstract

We study a phenomenological ansatz for merging next-to-next-to-leading order (NNLO) calculations with Monte Carlo event generators. We reweight them to match bin-integrated NNLO differential distributions. To test this procedure, we study the Higgs boson production cross-section at the LHC, for which a fully differential partonic NNLO calculation is available. We normalize PYTHIA and MC@NLO Monte Carlo events for Higgs production in the gluon fusion channel to reproduce the bin integrated NNLO double differential distribution in the transverse momentum and rapidity of the Higgs boson. These events are used to compute differential distributions for the photons in the $pp \to H \to \gamma\gamma$ decay channel, and are compared to predictions from fixed-order perturbation theory at NNLO. We find agreement between the reweighted generators and the NNLO result in kinematic regions where we expect a good description using fixed-order perturbation theory. Kinematic boundaries where resummation is required are also modeled correctly using this procedure. We then use these events to compute distributions in the $pp \to H \to W^+W^- \to l^+l^-\nu\bar\nu$ channel, for which an accurate description is needed for measurements at the LHC. We find that the final state lepton distributions obtained from PYTHIA are not significantly changed by the reweighting procedure.

arXiv:hep-ph/0604077v1 7 Apr 2006

I. INTRODUCTION

The search for the Higgs boson is a main objective of the LHC physics program. The ATLAS and CMS detectors are designed to detect a Higgs boson in the mass range from about 100 GeV up to at least 600 GeV. During the last 15 years, many Higgs boson signatures have been studied. For a detailed description of this effort we refer the reader to Refs. [1, 2, 3, 4]. If ATLAS and CMS function as designed, a discovery of a Standard Model Higgs boson over the entire mass range can be expected with luminosities of about 30 fb^{-1}.

It is interesting to study how well the mass, width, and couplings of a particle with the properties of a Higgs boson can be measured at the LHC, and how well these measurements can discriminate between the Standard Model and its viable extensions. The potential statistical accuracy for such measurements is usually assessed by computing experimental efficiencies using leading order (LO) parton shower Monte Carlo generators. However, these efficiency estimates cannot be expected to be accurate, especially in complicated signatures such as $pp \to H \to W^+W^-$.

It has been found that corrections beyond LO are particularly significant for Higgs boson production in the channel $gg \to H$. The next-to-leading-order (NLO) QCD corrections [5, 6] increase the cross-section by a factor of about 1.7-2 as compared to the LO result. A few years ago, the inclusive cross-section was computed in the large m_{top} limit with NNLO accuracy [7, 8, 9]. The new corrections increase the NLO cross-section by another $20-25\%$. Very recently, some threshold-enhanced N^{3}LO terms were also computed [10], changing the NNLO result by less than 5%. These computations show that the Higgs boson cross-section can be reliably estimated only after many orders in perturbation theory have been considered. It is therefore necessary to account for higher order corrections in a realistic analysis of the Higgs boson signal.

Recently, a program FEHIP that describes Higgs boson production in gluon fusion was developed [11, 12]. FEHIP computes the cross-section and fully differential distributions for Higgs boson production at NNLO in QCD. Arbitrary cuts can be imposed on partonic jets and on the decay products of the Higgs boson. FEHIP does not have an implementation of a parton shower and a hadronization algorithm. This creates a few shortcomings, since it is not possible to apply cuts at the hadron level or to generate events for a detector simulation. In addition, regions of phase-space close to kinematic boundaries can not be described reliably in fixed-order calculations. This feature manifests itself in large perturbative corrections at special kinematic regions, such as the low Higgs $p_\perp$ region.

To overcome these characteristic problems of fixed order perturbative computations, the resummation of soft gluon effects to all orders in perturbation theory must be performed. This resummation may be obtained using analytical techniques [13, 14]. Alternatively, these effects are also included in parton shower Monte Carlo programs. Novel approaches [17, 18, 19, 20] merge cross-sections computed in fixed order perturbation theory with these LO event generators, such as PYTHIA [15] and HERWIG [16]. Very significant progress has been achieved, and the pioneering Monte-Carlo event generator MC@NLO [17] combines consistently NLO perturbative calculations with HERWIG for a number of processes at hadron colliders. Unfortunately, no method exists which merges parton shower algorithms with NNLO partonic cross-sections consistently. This is desirable for processes with large perturbative corrections.

It is possible to incorporate NNLO corrections into realistic analyses of experimental signatures in an approximate way by multiplying probabilities of events in a parton shower

Monte Carlo simulation by so-called K-factors. These factors force the Monte Carlo output to agree with certain observables computed in perturbative QCD. This technique is called event reweighting. The simplest version of this technique is a multiplication of the Monte Carlo output by a constant factor so that the total cross-sections computed perturbatively and with the reweighted Monte-Carlo simulation agree.

Re-scaling Monte Carlo output by a constant factor does not guarantee an agreement between perturbative and Monte Carlo results for differential distributions, since perturbative corrections do depend on kinematic variables and vary across the phase-space. A better job may be done if the Monte Carlo output and the perturbative calculation are matched at the differential level [21]. A point-by-point reweighting of the Monte-Carlo throughout the available phase-space is not possible, since infrared divergences would produce divergent weights. We must instead select a realistic set of observables to match, and then check if the reweighted simulation gives a reliable prediction for other observables.

In this paper we study the reweighting procedure for Higgs boson production in the gluon fusion channel at the LHC. We match the Monte-Carlo output of both PYTHIA and MC@NLO to distributions that depend only on the Higgs boson kinematics, which is a simple and obvious way of reweighting the Monte Carlo output. We match to a double differential distribution in the Higgs boson transverse momentum and rapidity. This distribution is chosen both for its simplicity and because it allows us to decouple the Higgs boson decay chain from the Higgs boson production. However, the kinematics of accompanying QCD radiation is totally ignored in the reweighting process. This ignorance is not a problem if hadronic radiation is treated fairly inclusively by cuts applied to a process of interest; however, if a detailed description of the hadronic radiation becomes relevant, the reweighting procedure may lead to inaccurate results. A particular example of a situation when this happens is the jet veto on transverse momenta of hadronic jets; we discuss it in detail in Section II.

The paper is organized as follows. In Section II we introduce the reweighting procedure and discuss in detail differential distributions in the reaction $pp \rightarrow H + X$. We first study the reweighting procedure at NLO by comparing the fixed order result with PYTHIA and MC@NLO. We present an example in which the reweighting procedure fails to produce accurate acceptances: when a jet veto is imposed on the transverse momenta of extra QCD radiation. We explain how this problem is ameliorated at NNLO.

We then apply the reweighting approach to estimate the NNLO effects for the channels $pp \rightarrow H \rightarrow \gamma\gamma$ and $pp \rightarrow H \rightarrow W^+W^- \rightarrow l^+\nu l^-\bar{\nu}$. We first reweight PYTHIA and MC@NLO events in the $pp \rightarrow H \rightarrow \gamma\gamma$ channel. We compute the accepted cross-section and differential distributions which have a potential discriminating power from the di-photon irreducible background [12, 25, 26]: the average $p_m = (p_\perp^{\gamma_1} + p_\perp^{\gamma_2})/2$ transverse momentum distribution and the pseudorapidity difference $\eta^* = |\eta^{\gamma_1} - \eta^{\gamma_2}|/2$ of the two photons. We find an excellent agreement between the reweighted PYTHIA and MC@NLO events for all observables. The di-photon channel is a testing ground for the reweighting procedure, since we can compare the results with the NNLO predictions of FEHIP for the same observables. We find that accepted cross-sections agree better than 1%. The p_m, η^* distributions also agree very well away from kinematic thresholds. Near these boundaries, they reproduce the correct resummed behavior of the parton-shower Monte Carlo simulations.

We next study the $pp \rightarrow H \rightarrow W^+W^- \rightarrow l^+l^-\nu\bar{\nu}$ channel. Ref. [21] already employed a reweighting technique in order to study the effect of perturbative corrections in this channel by matching the PYTHIA output to the resummed $p_\perp$ spectrum of the Higgs boson [14].

An optimal set of cuts for isolating a Higgs signal in this channel was introduced and studied in [22]. A study of this channel with higher-order QCD corrections included was presented in [27], where both the signal and $qq \to WW$ background were included using a reweighting technique. The analysis in Section II of the accuracy achievable by reweighting PYTHIA for processes with a jet veto cut implies that at least *shapes* of distributions can be predicted reliably. Hence, we calculate various lepton distributions in the reaction $pp \to H \to W^+W^- \to l^+l^-\nu\bar{\nu}$. Interestingly, the reweighting turns out to be largely irrelevant for these distributions and the prediction of reweighted PYTHIA and standard PYTHIA agree very well.

II.   THE REWEIGHTING TECHNIQUE FOR $pp \to H + X$

A.   The reweighting procedure

The cross-sections computed with generator $G = \{$PYTHIA, MC@NLO$\}$ for the process $pp \to H + X$ are

$$\sigma^G = \sum_m \int d\Pi_m f_m^G \left(\{p_i\}\right) \mathcal{O}_m \left(\{p_i\}\right), \tag{1}$$

where we sum over all final-state multiplicities m, and integrate the events f_m^G over the phase-space variables $d\Pi_m$ of all $i \leq m$ particles in the final state. The function $\mathcal{O}_m$ selects the kinematic configurations to be accepted in the measured cross-section. The events depend implicitly on the renormalization and various factorization scales.

The simplest observable is the total cross-section σ_{incl}^G, corresponding to $\mathcal{O}_m \left(\{p_i\}\right) = 1$. It is a well-known fact that standard event generators fail to predict total cross-sections reliably. As an example we set the mass of the Higgs boson to $m_H = 165$ GeV, and the renormalization and factorization scales to $\mu_R = \mu_F = m_H/2$. We use the generators PYTHIA version 6.325 with a Q^2 ordered parton shower and MC@NLO version 3.2 For PYTHIA we use the MRST2001 LO set of parton-distribution functions, while for MC@NLO we use the corresponding NLO set. In MC@NLO, the scale choice $\mu_R = \mu_F = m_H/2$ is also used, instead of the default setting. The resulting PYTHIA and MC@NLO cross-sections are

$$\sigma_{\text{incl}}^{\text{PYTHIA}} = 12.20 \, \text{pb} \qquad \sigma_{\text{incl}}^{\text{MC@NLO}} = 23.92 \, \text{pb}. \tag{2}$$

The corresponding fixed-order NNLO cross-section is

$$\sigma_{\text{incl}}^{\text{NNLO}} = 27.78 \text{pb}. \tag{3}$$

The large differences between the PYTHIA, MC@NLO and NNLO cross-sections reflect the fact that the NLO and NNLO perturbative corrections are very significant.

A consistent method for merging fixed-order perturbative calculations and parton-shower algorithms is only formulated at NLO in perturbation theory, and is implemented in MC@NLO. A similar procedure beyond NLO is not yet available. Nevertheless, we would like to incorporate the large perturbative corrections into the event generators. In this paper, we adopt a pragmatic approach to solve this problem. We multiply the integrand in Eq.(1) with a function K^G,

$$\sigma^{R(G)} = \sum_m \int d\Pi_m f_m^G \left(\{p_i\}\right) K^G \left(\{p_i\}\right) \mathcal{O}_m \left(\{p_i\}\right), \tag{4}$$

in order to reweight the events f_m^G,

$$f_m^G \rightarrow f_m^{R(G)} = f_m^G K^G.$$

The reweighting factors K^G model the effect of higher order corrections through a certain order in perturbation theory. We determine the factors K^G by requiring that Eq.(4) reproduces the fixed-order perturbative results for selected distributions,

$$\sigma^{R(G)} \left(\mathcal{O}_{\mathrm{special}} \right) = \sigma^{\mathrm{PT}} \left(\mathcal{O}_{\mathrm{special}} \right). \tag{5}$$

We emphasize that Eq.(4) is an approximate ansatz to describe effects of higher order corrections in the absence of a rigorous treatment. Strictly speaking, higher order corrections do depend on parton multiplicities. For example, $pp \rightarrow H + 0$ jets is renormalized differently compared to, $pp \rightarrow H + 1$ jet. This feature is ignored in Eq.(4), where the reweighting factors K_G do not depend on the multiplicities m. A more detailed version of reweighting would not be universal, because matrix elements with fixed multiplicities of partons are divergent in perturbation theory. Independent renormalization of events with different multiplicities has to depend on a globally-defined set of cuts, e.g. the jet finding algorithm. This invalidates the unweightedness of events, the single most important feature of parton shower Monte Carlo event generators. We will see the errors in the reweighting procedure caused by neglecting the dependence on parton multiplicities later in this section, when we compare reweighted PYTHIA at NLO with MC@NLO.

Having pointed out the approximate nature of the reweighting procedure, we discuss a choice of a suitable distribution for which the agreement of a Monte Carlo generator and the perturbative calculation can be imposed. Since, as we discussed in the previous paragraph, the reweighting ansatz is unsuitable for resolving the structure of QCD radiation, we use the kinematic variables which describe the Higgs boson. Since, up to an angle in a plane transverse to the collision axis, the Higgs boson kinematics is determined by its transverse momentum $p_\perp$ and rapidity Y, we normalize the events f_m^G to the magnitudes and shapes of the NNLO bin-integrated double differential distributions in Y and $p_\perp$. We expect that such a normalization renders the events more realistic in predicting other observables of the process. Without a technique for combining NNLO results with parton showering in the spirit of MC@NLO, this is the best way we have of combining these calculations with event generators. Note that we are not changing the properties of the radiation produced by the Monte Carlo generators. We are only changing the normalization of these events to reproduce certain distributions. The reweighted generators therefore do not better describe events with multiple hard radiations.

We choose

$$\mathcal{O}_{\mathrm{special}} = \left\{ \begin{array}{l} 1, \text{ if } p_\perp \in \left[p_\perp^j, p_\perp^{j+1} \right] \text{ and } Y \in \left[Y^i, Y^{i+1} \right] \\ 0, \text{ otherwise,} \end{array} \right\} \tag{6}$$

and define the K-factors as

$$K_{ij}^G := K^G(\{p_f\}) = \frac{\Delta\sigma_{ij}^{\mathrm{PT}}}{\Delta\sigma_{ij}^G} \quad \text{if } p_\perp \in \left[p_\perp^j, p_\perp^{j+1} \right] \text{ and } Y \in \left[Y^i, Y^{i+1} \right], \tag{7}$$

where $\Delta\sigma_{ij}^{\mathrm{PT},G}$ are the accepted cross-section computed at fixed order perturbation theory and with the generator G, respectively. The values of the bin boundaries $p_\perp^j$ and Y^i are chosen in such a way that they capture the shape of the Higgs $p_\perp$ and rapidity distributions

and span the allowed kinematic range for Y and $p_\perp$. In what follows we always set the renormalization and factorization scales to $\mu_R = \mu_F = m_H/2$, since this choice is known to yield a perturbative series with faster convergence [8].
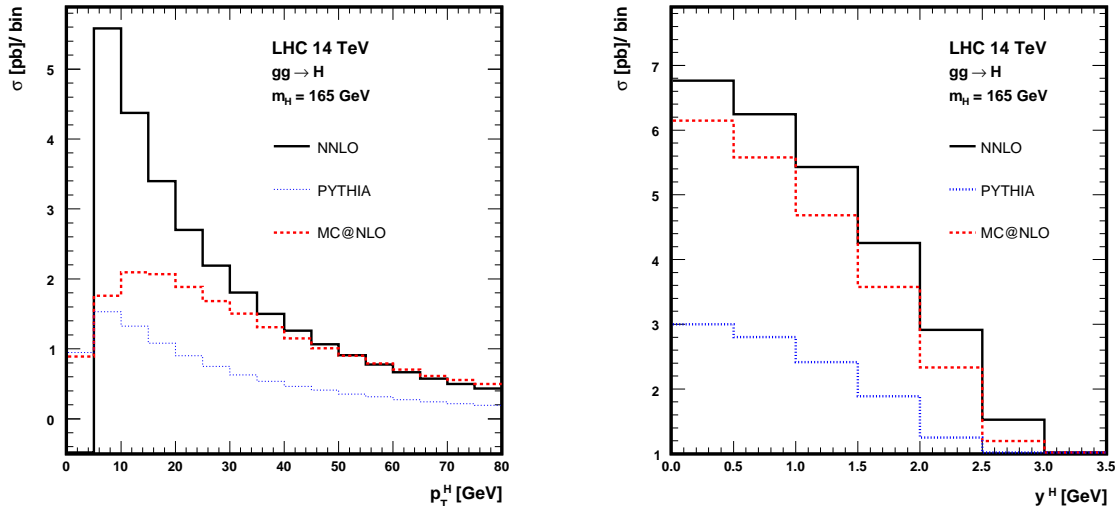

FIG. 1: Distributions of the Higgs transverse momentum (left) and rapidity (right).

We point out that at NLO the $p_\perp$ and Y variables completely constrain the kinematics of the process $pp \to H + X$. At NNLO, new tree level processes $pp \to H + i + j$ with two partons in the final state require additional phase-space variables in order to determine the kinematics of partonic radiation. Our reweighting functions K^G are independent of these additional variables. This may create a problem in case there are important cuts on the hadronic radiation.

The choice of the bin boundaries in $p_\perp$ of the Higgs boson is a subtle issue. Some of the standard cuts that we need to apply in Higgs boson production processes have a strong dependence on the $p_\perp$ of the Higgs boson. For example, in the WW decay channel it is important to have a phenomenologically realistic model for the low and intermediate $p_\perp$ region since after cuts most of the signal comes from the region of low Higgs $p_\perp$. The Higgs $p_\perp$ distribution in this region is not correctly described in fixed-order calculations. Logarithms of the form $\log p_\perp/m_H$ become large and require a resummation. Nevertheless, fixed order calculations for cross-sections integrated over $p_\perp$ of the Higgs boson are still viable, provided that the integration region is sufficiently broad.

In Fig. 1 we show the $p_\perp$ distributions for the fixed-order NNLO calculation, PYTHIA and MC@NLO. We observe that the perturbative NNLO result breaks down at small $p_\perp$. The $p_\perp$ spectrum of PYTHIA is peaked at lower $p_\perp$ than MC@NLO. The most reliable spectrum at low $p_\perp$ is obtained with resummation [14]. To avoid problems associated with the low-$p_\perp$ region in fixed order perturbative calculations, we choose the first $p_\perp$ bin, $[p_\perp^0 = 0, p_\perp^1]$, in Eq.(6) to be sufficiently broad by taking $p_\perp^1 = 25$ GeV. Therefore, for $p_\perp < 25$ GeV, we reweight all events with a uniform factor, maintaining the shape of the $p_\perp$ distribution provided by the generator G. Above 25 GeV, we trust the shape of the perturbative result

and reweight in bins of $5\,\mathrm{GeV}$

$$p_\perp^0 = 0, \quad p_\perp^1 = 25\,\mathrm{GeV}, \quad p_\perp^i = (25 + (i-1)5)\,\mathrm{GeV},$$

and

$$Y^j = 0.5(j-1)\,, \; j = 1\ldots 9.$$

Note that this reweighting procedure leads to a discontinuity at $p_\perp = p_\perp^1$ in the reweighted $p_\perp$ spectrum computed with the generator G. The choice of $p_\perp^1$ is ambiguous; however, it turns out that this ambiguity is largely irrelevant in practice. In what follows we take the first bin in $p_\perp$ to be $[0 - 25\;\mathrm{GeV}]$, unless explicitly stated otherwise.

At this point it is worth investigating if just a single, constant K-factor is sufficient for accurate reweighting. To do so, we investigate the dependence of the reweighting factors K^G in Eq.(4) on the $p_\perp$ and rapidity and find that $K^G(p_\perp, Y)$ can vary significantly in different rapidity and $p_\perp$-bins. For PYTHIA, we find K-factors ranging from 1.8 to 3.5, while for MC@NLO the K-factors can vary from 0.7 to 1.6 in bins with a significant number of events. For illustration, in Fig. 2 we show the reweighting factors for the $p_\perp$ distribution, after we integrate over rapidity. We also show the reweighting factors as a function of Y, after integrating over $p_\perp$. The shape of the K-factors in the two variables is not uniform, indicating that a naive multiplication with a uniform K-factor from the total cross-section may not be adequate. Having discussed the reweighting technique in general, we now study it in the process $pp \rightarrow H + X$ at both NLO and NNLO.
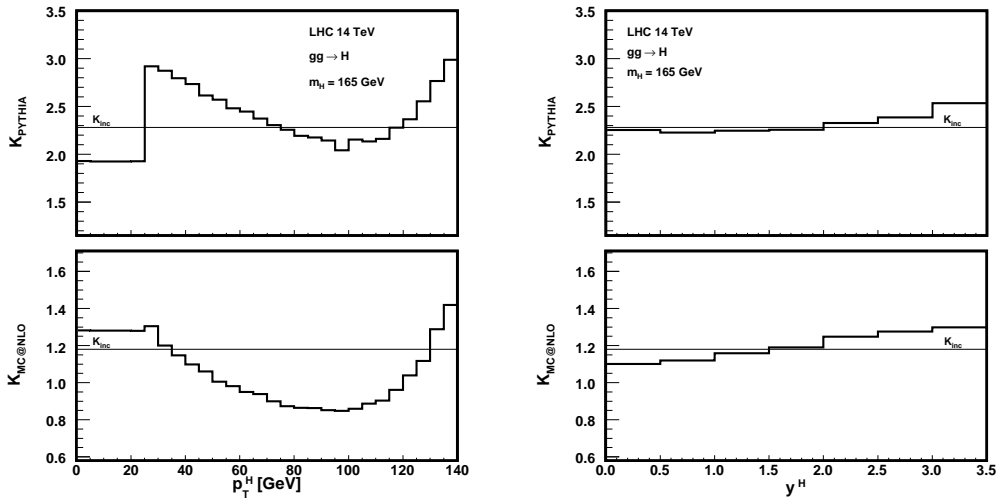

FIG. 2: The reweighting factors integrated over rapidity for PYTHIA and MC@NLO as functions of the Higgs $p_\perp$ (left). The reweighting factors, integrated over $p_\perp$, as functions of rapidity (right). The inclusive K-factor for the total cross-section is also shown on both plots as a horizontal line.

B. The reweighting at NLO and NNLO

We now apply the reweighting procedure to PYTHIA and MC@NLO to study $pp \rightarrow H + X$. MC@NLO is a Monte Carlo event generator that accommodates NLO perturbative

calculations for a wide range of processes. Its important feature is that the parton shower is combined with NLO matrix elements consistently, without double counting. PYTHIA is an event generator based on leading order matrix elements, so that hadronic radiation is generated primarily through the parton shower.

We begin our study by checking how well reweighting works at NLO. We check how well the procedure describes Higgs boson production when a jet veto is imposed. This tests whether the neglect of the additional hadronic radiation in our reweighting ansatz is problematic. Phenomenologically, this cut is needed in the $pp \to H \to W^+W^- \to l^-l^+\bar{\nu}\nu$ channel to isolate the signal from background. The inclusive cross sections for both PYTHIA and MC@NLO are given in Eq.(2), while $\sigma_{\rm incl}^{\rm NLO} = 23.99$ pb. We impose a jet veto of $p_\perp < 30$ GeV, and we define jets with a cone algorithm using a cone size $R = 0.4$. The cross sections after the jet veto has been imposed are

$$
\sigma_{\rm acc}({\rm pb}) = \begin{cases} 6.12, & {\rm PYTHIA}; \\ 12.09, & {\rm MC@NLO}; \\ 14.48, & {\rm R^{NLO}(PYTHIA)}; \\ 16.34, & {\rm NLO}. \end{cases} \tag{8}
$$

The acceptances, defined as the ratios of the accepted cross sections over the inclusive cross sections, are

$$
A = \begin{cases} 0.50, & {\rm PYTHIA}; \\ 0.51, & {\rm MC@NLO}; \\ 0.60, & {\rm R^{NLO}(PYTHIA)}; \\ 0.68, & {\rm NLO}. \end{cases} \tag{9}
$$

We observe a very large disagreement, of order 30%, between the acceptances obtained using the generators and the fixed order NLO result. What is occurring here is that this observable is very sensitive to the properties of the QCD radiation. Multiple partonic emissions are required to generate the correct jet $p_\perp$ spectrum, and the NLO result contains only a single partonic emission. The $p_\perp$ spectrum of this additional parton is generated for the first time at NLO, and is therefore not accurately predicted at this order in the perturbative expansion. We note that reweighting PYTHIA to the NLO result spoils the agreement between its acceptance and that computed with MC@NLO.

To check that multiple emissions are indeed important, we present below the jet multiplicites for both PYTHIA and MC@NLO before a jet veto is imposed. We study the cross-section both inclusively and with the restriction $p_\perp^H > 30$ GeV, to show that multiple emissions are required to obtain correctly even the high $p_\perp$ events. We present the fraction of events with $N = 0, 1, 2, 3, 4$, or more jets in Table I. Note that we require a jet to have $p_\perp > 20$ GeV, so events without jets are possible. Over half of the events in the high $p_\perp^H$ tail coming from PYTHIA and MC@NLO contain multiple emissions, indicating that the description of the hadronic radiation coming from the single emission at NLO is unlikely to be very accurate. We can also see this by studying the Higgs $p_\perp$ spectrum, shown in the left panel of Fig. 3. The single hard partonic emission is equivalent in the fixed order NLO result and in MC@NLO. The mismatch between them in the high $p_\perp^H$ tail is caused by showering. The importance of the multiple emissions is made explicit in the right panel of Fig. 3, where the $p_\perp^H$ from MC@NLO when only a single jet is observed is compared to the NLO calculation. The distributions agree very well in the high $p_\perp^H$ region for this single emission case, again indicating the need for multiple emissions to correctly generate this spectrum.

	Inclusive		$p_\perp^H > 30$	
	PYTHIA	MC@NLO	PYTHIA	MC@NLO
$N = 0$	0.365	0.39	0.055	0.090
$N = 1$	0.335	0.345	0.40	0.465
$N = 2$	0.18	0.17	0.31	0.275
$N = 3$	0.080	0.060	0.15	0.105
$N = 4$	0.030	0.020	0.055	0.040
$N > 4$	0.010	0.015	0.030	0.025

TABLE I: Fraction of events with $N = 0, 1, 2, 3, 4$ or more jets for inclusive Higgs boson production and Higgs boson production with $p_\perp^H > 30$ GeV in PYTHIA and MC@NLO.

FIG. 3: The Higgs boson $p_\perp$ spectrum for NLO, MC@NLO, and PYTHIA reweighted (left panel); comparison of the Higgs boson $p_\perp$ at NLO, and with MC@NLO when only a single jet is observed (right panel).

We next study what happens when we perform the reweighting at NNLO. We use FEHIP to obtain these results. The inclusive NNLO cross section is given in Eq.(3). We include the reweighting of MC@NLO to the NNLO double differential distribution. The accepted cross sections for NNLO and the reweighted event generators are

$$
\sigma_{\rm acc}({\rm pb}) = \begin{cases} 13.1, & {\rm R^{NNLO}(PYTHIA)}; \\ 14.9, & {\rm R^{NNLO}(MC@NLO)}; \\ 14.9, & {\rm NNLO}. \end{cases} \tag{10}
$$

The acceptances are

$$A = \begin{cases} 0.47, & R^{NNLO}(\text{PYTHIA}); \\ 0.54, & R^{NNLO}(\text{MC@NLO}); \\ 0.54, & \text{NNLO}. \end{cases} \qquad (11)$$

We observe a much better agreement with the NNLO reweighting. R(PYTHIA), R(MC@NLO) and the fixed order NNLO result all agree with the PYTHIA and MC@NLO acceptances within 6%. The NNLO result contains two partons in the final state, which gives a more realistic accounting of the QCD radiation. It also contains the first radiative correction to the single parton $p_\perp$ spectrum. The $p_\perp$ spectrum obtained at NNLO is in better agreement with MC@NLO, as seen in Fig. 1. A comparison of the $p_\perp$ spectrum from the reweighted generators with the resummed $p_\perp$ distribution of [28] is presented in Fig. 4. There is good agreement between $R^{NNLO}(\text{MC@NLO})$ and the resummed calculation. $R^{NNLO}(\text{PYTHIA})$ agrees with the intermediate and large $p_\perp$ portion of the resummed distribution, while there is a slight discontinuity induced by the first bin reweighting in the low $p_\perp$ region. We conclude that even in the presence of significant cuts on the jets in the final-state, the simple reweighting of the Higgs boson double differential distribution at NNLO describes the acceptances well. In addition, since the NNLO result produces the correct normalization and contains drastically reduced scale dependences, we believe that reweighting MC@NLO with the fully differential NNLO result of FEHIP provides a very accurate prediction for the Higgs boson signal at the LHC.

As a final check, we compute the rapidity distribution of the Higgs boson using FEHIP and the reweighted event generators. The result is shown in fig. 5. We observe that imposing the jet veto maintains the matching of this distribution.
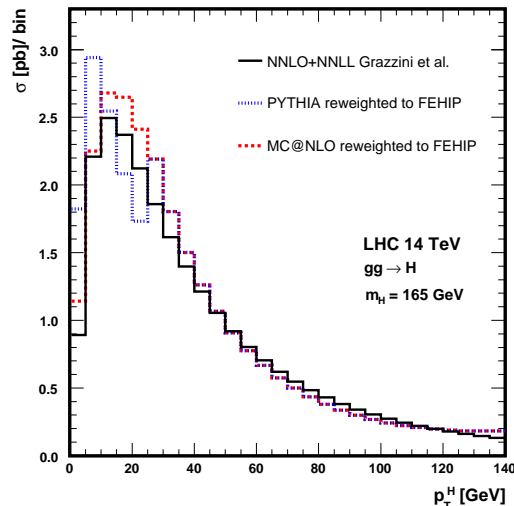

FIG. 4: The Higgs boson $p_\perp$ spectrum from a resummed calculation, MC@NLO reweighted and PYTHIA reweighted.

Motivated by the success of the NNLO reweighting procedure, we now allow the Higgs to decay and study predictions for the $pp \to H + X \to \gamma\gamma + X$ and $pp \to H \to W^+W^- \to l^-l^+\bar{\nu}\nu$ channels.
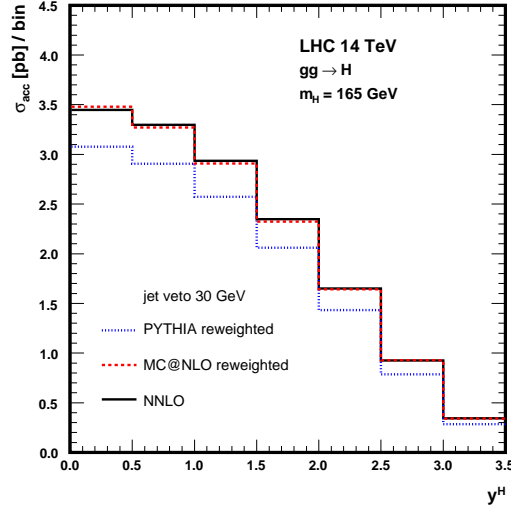
FIG. 5: The Higgs boson rapidity distribution with a jet veto of 30 GeV applied for NNLO, MC@NLO reweighted and PYTHIA reweighted.

III. THE DI-PHOTON CHANNEL

We first use the reweighting procedure to compute the cross-sections for observables in the $pp \to H + X \to \gamma\gamma + X$ channel. The standard cuts on the two photons are

- $p_\perp^{\gamma_1} > 40 \, \text{GeV}$ and $p_\perp^{\gamma_2} > 25 \, \text{GeV}$;

- $|\eta^{\gamma_{1,2}}| < 2.5$;

- $E_{\text{hadr}} < 15 \, \text{GeV}$ in cones of size $R = 0.4$ around each photon.

The two-photon channel is useful for additional checks of the reweighting approach. Because the $H \to \gamma\gamma$ decay is included in the FEHIP program, we can compare observables computed with R(PYTHIA) and R(MC@NLO) directly with NNLO results.

We first compare the various results for the accepted cross-sections after applying the standard cuts. We choose a Higgs mass $m_H = 120 \, \text{GeV}$ and set the renormalization and factorization scales to $\mu_R = \mu_F = m_H/2$. For the $H \to \gamma\gamma$ branching ratio we assume the value $\text{Br}(H \to \gamma\gamma) = 0.002205$, which we obtain from HDECAY [24]. We find the following cross-sections for the di-photon signal:

	PYTHIA	MC@NLO	R(PYTHIA)	R(MC@NLO)	NNLO
σ_{acc}[fb]	36.8	60.3	65.3	66.9	66.4

The PYTHIA, MC@NLO and the NNLO results differ significantly, reflecting again the large NLO and NNLO corrections. However, the reweighted cross-sections agree within 2.5%, and differ from the NNLO result only by -1.7% for R(PYTHIA) and $+1.0\%$ for R(MC@NLO).

The effect of the cuts on the accepted cross-section in the two-photon channel is rather insensitive to the choice of generator, and the reweighting procedure reproduces the NNLO

11

results reliably. This is an expected result, since in the di-photon decay the experimental cuts do not resolve the structure of the hadronic system that recoils against the Higgs boson.

We next compare the reweighted results and the NNLO predictions for more complicated observables in the di-photon channel. In Refs [12, 25, 26] the distribution of the pseudorapidity difference of the two-photons $y^* = 1/2\,|\eta^{\gamma_1} - \eta^{\gamma_2}|$ was proposed as a discriminator to separate the signal from the prompt photon background. In Fig. 6 we present the y^*-distribution for PYTHIA and MC@NLO, as well as for the reweighted generators and at NNLO. We observe that the reweighted and the NNLO distributions agree reasonably well. At the boundary of the kinematic region $y^* \geq 0.96$, the NNLO distribution is non-monotonic. This kinematic region corresponds to a vanishing leading order cross-section, and the perturbative result must be resummed to all orders. PYTHIA and MC@NLO do not suffer from this problem since parton showers perform such resummations. The reweighted generators maintain the resummed behavior at the kinematic boundary and reproduce the fixed order result elsewhere.
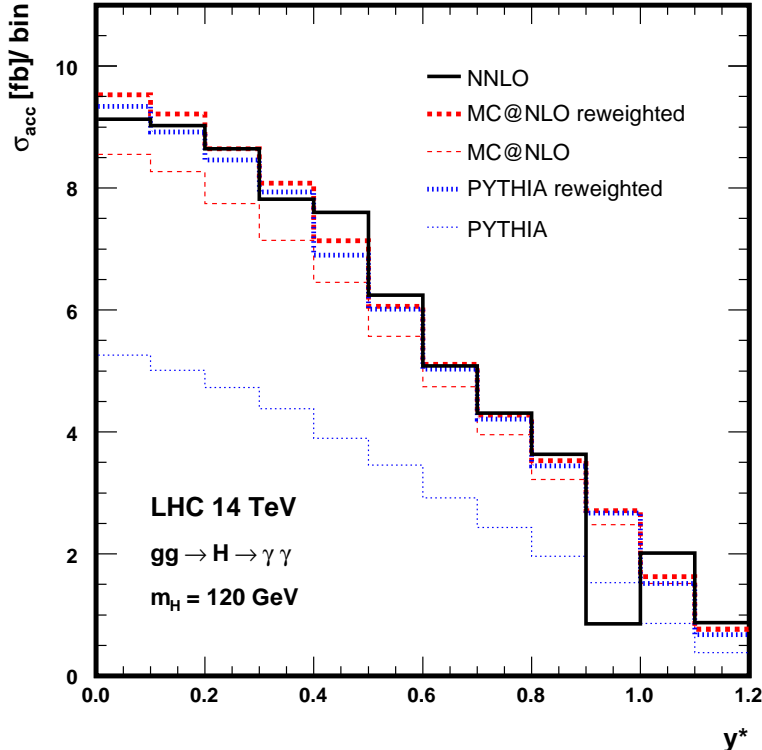

FIG. 6: The pseudorapidity difference y^*-distribution for di-photon events. We compare PYTHIA and MC@NLO with the reweighted generators and NNLO.

We now study the average $p_\perp$ distribution of the two-photons, $p_m = 1/2(p_\perp^{\gamma_1} + p_\perp^{\gamma_2})$ [12, 26]. At leading order in perturbation theory the cross-section is zero for $p_m > m_H/2$. The distribution at higher orders retains a characteristic peak at $p_m \sim m_H/2$. In Fig. 7 we show the distribution for PYTHIA, MC@NLO, and FEHIP, and also after reweighting. We
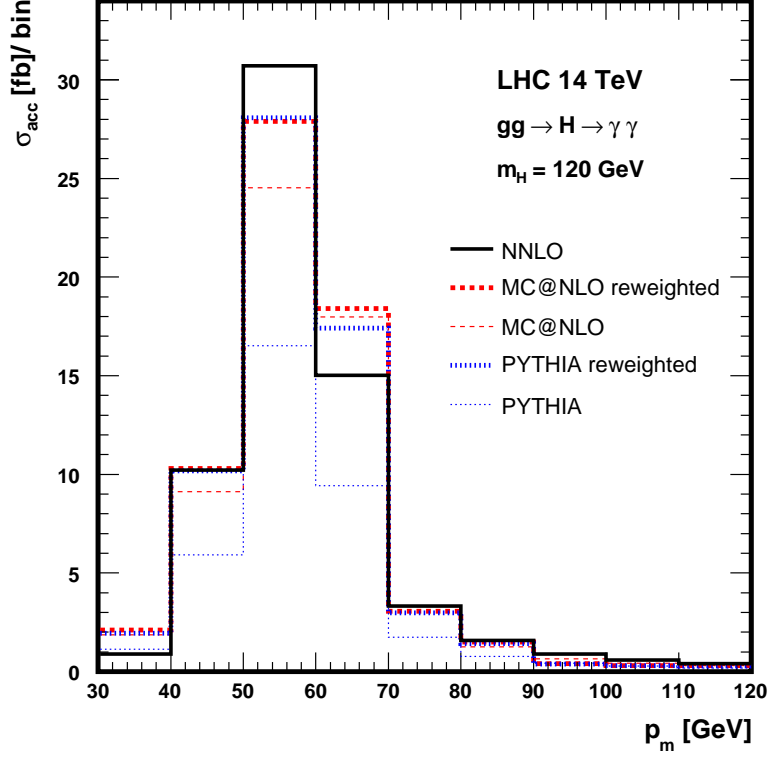
FIG. 7: The average transverse momentum p_m-distribution for the two photons. We compare PYTHIA and MC@NLO with the reweighted generators and NNLO.

again find a very good agreement between the R(PYTHIA) and R(MC@NLO) results. The NNLO distribution agrees very well away from the peak at $p_m \sim m_H/2$. As expected, the NNLO result at the peak is substantially different because this region cannot be predicted accurately in fixed-order perturbation theory, and requires resummation. The reweighted generators do a reasonably good job at maintaining the appropriate resummed behavior at the peak.

The ratio of the di-photon cross-sections computed with the reweighted and the leading order generators is very similar to the NNLO K-factor for the total cross-section. The reweighting of the event generators with a constant factor could also yield realistic results for the di-photon cross-section after applying the standard cuts. It is interesting to investigate if a constant K-factor is also sufficient for reweighting differential distributions. We have already seen that this would not be satisfactory for the $p_\perp$ and rapidity distributions for the Higgs boson in Fig. 2. To investigate this, we compute the effective K-factors for each bin of the y^* and p_m distributions,

$$K_G(\text{bin}) = \frac{\Delta\sigma^{R(G)}(\text{bin})}{\Delta\sigma^G(\text{bin})}. \tag{12}$$
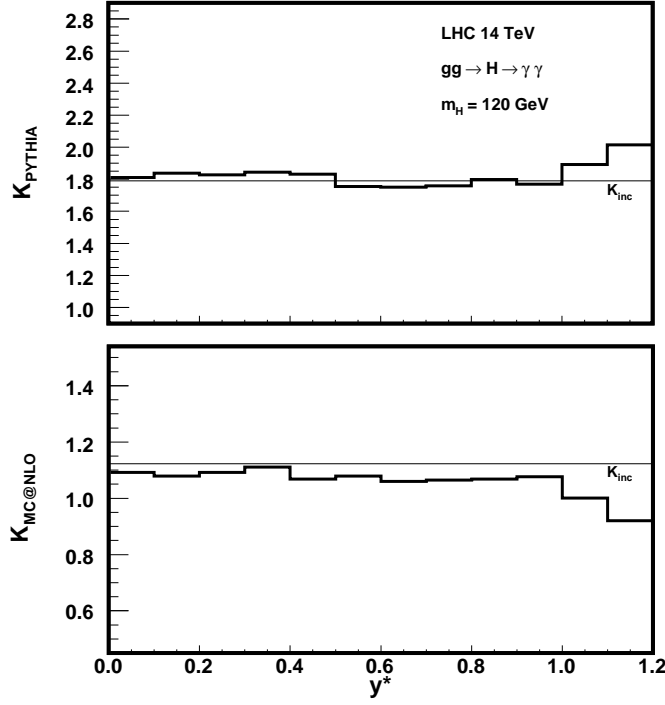
13

FIG. 8: The effective K-factors as a function of y^* for PYTHIA and MC@NLO.

In Fig. 8 we show that the effective K-factors in each bin of the y^* distribution do not vary significantly from the inclusive K-factor. However, in the average photon $p_\perp$ distribution of Fig. 9, the effective K-factors for high p_m bins away from the peak are not uniform, although the large kinematic variations occur in bins with few events.

IV. THE $W^+W^- \to l^+l^-\nu\bar{\nu}$ CHANNEL

In this Section we study the reaction $pp \to H \to W^+W^- \to l^+l^-\nu\bar{\nu}$. This signal can be distinguished from the main background process $pp \to W^+W^-$ by applying a jet veto, requiring a small opening angle between the two charged leptons in the transverse plane, and applying some additional kinematic cuts [22, 23].

In the remainder of this Section, we present new results with the R(PYTHIA) generator in the $H \to W^+W^- \to l^+l^-\nu\bar{\nu}$ decay channel. The observables that we consider probe the momenta of the final-state leptons. The W^+W^- decay chain is not yet implemented in FEHIP, and a comparison with NNLO is not possible. In addition, the Herwig event-generator, which is a basic component of MC@NLO, does not have an implementation of the same decay with full spin correlations. Therefore, we will not present any leptonic observables with R(MC@NLO).

We first present a study of the K-factor for the $H \to W^+W^- \to l^+l^-\nu\bar{\nu}$ channel. Using R(PYTHIA), we can obtain a description of the Higgs boson rapidity distribution valid to NNLO, and examine the effect of this rapidity dependence. The effective K-factor integrated over the whole region after all $H \to WW$ cuts are applied is 2.098. If we reweight PYTHIA to only the $p_\perp$ spectrum of the Higgs boson, we find an effective K-factor of 2.02. The
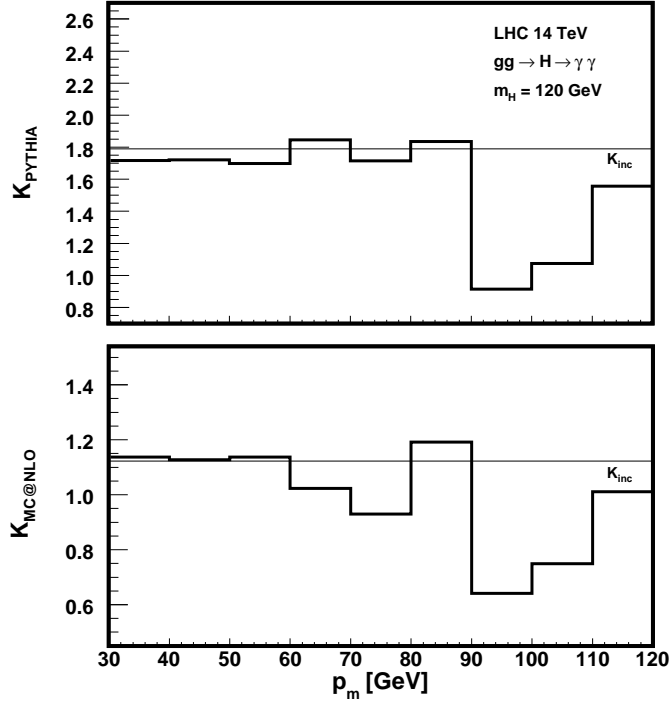
FIG. 9: The effective K-factors as a function of the p_m distribution for PYTHIA and MC@NLO.

$(p_\perp, Y)$ dependent effective K-factor is 10% lower than the fully inclusive K-factor of 2.28, while the K-factor coming from only reweighting to the $p_\perp$ distribution is 13% lower than the inclusive K-factor, comparable with the results from [28]. The effect of the rapidity dependence is therefore less than 3%.

We now employ R(PYTHIA) to study distribution shapes in $pp \to H \to W^+W^- \to l^+l^-\nu\bar{\nu}$. We normalize each result to the integrated cross-section subject to the appropriate cuts. Since the distributions studied do not probe the hadronic radiation, we expect them to be very well described by R(PYTHIA).

In Fig 10 we plot the minimum and maximum transverse momentum distributions of the detected leptons for PYTHIA and R(PYTHIA) events. These distributions are characteristic of the Higgs signal and can be used to discriminate from the background. We observe that the reweighting does not change the shape of distributions. An application of a constant K-factor would lead to the same results. However, the appropriate K-factor is the effective one of 2.098 discussed at the beginning of this section, which is 10% lower than the fully inclusive K-factor.

V. CONCLUSIONS

In this paper, we have presented a phenomenological approach to including NNLO corrections in event generators such as PYTHIA or MC@NLO. Without an extension of the MC@NLO procedure to NNLO, this offers the best way of combining parton showering and hadronization with NNLO calculations. We study this procedure for Higgs boson production at the LHC, since the fully differential NNLO calculation is available in the program FEHIP.
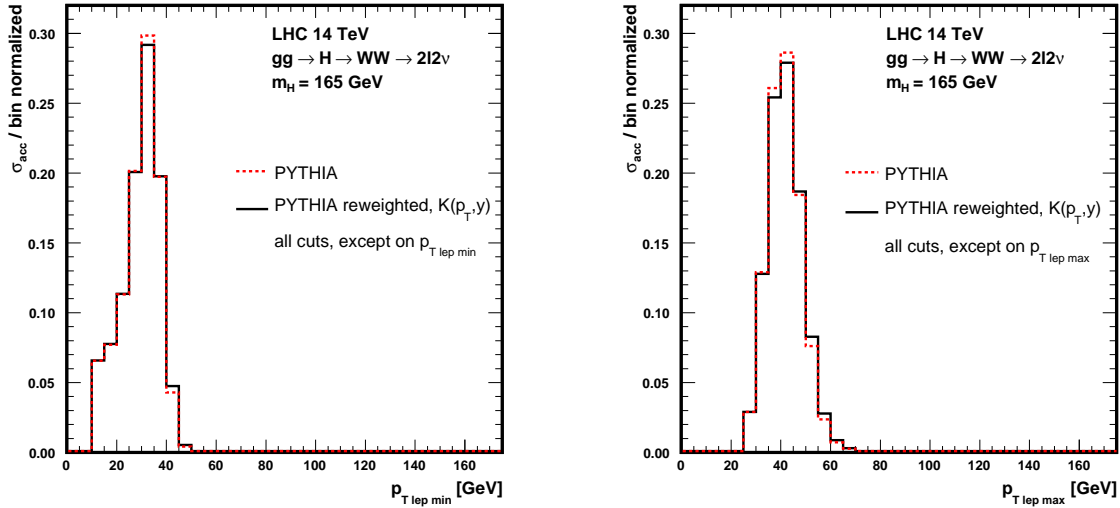
FIG. 10: The minimum (left) and maximum (right) transverse momentum of the two leptons computed with PYTHIA and R(PYTHIA).

We reweight the Monte-Carlo events of PYTHIA and MC@NLO to match the bin-integrated NNLO double differential distribution in the Higgs $p_\perp$ and rapidity. We then study how well distributions of the Higgs boson decay products are predicted by this reweighting procedure. We note that the K-factors that describe the reweighting of both PYTHIA and MC@NLO exhibit significant kinematic dependences, so that the use of a single constant K-factor may not be adequate.

We first study the reweighting procedure for the process $pp \rightarrow H + X$, without decays of the Higgs boson. The K-factors that describe the reweighting of both PYTHIA and MC@NLO depend significantly on the Higgs boson transverse momentum, and non-negligibly on its rapidity. We test how well reweighting reproduces a fully consistent merging of fixed-order calculations with parton showering by reweighting PYTHIA at NLO and comparing to MC@NLO. We find large discrepancies when a jet veto is imposed. This indicates that the single parton emission present in the NLO calculation is insufficient to correctly describe cuts where the hadronic structure is probed. The reweighting in the presence of a jet veto works much better at NNLO, where two partonic emissions are present in the final state. This indicates the importance of extending perturbative calculations to NNLO in order to obtain a reasonable description of the additional radiation.

We then examine the decay channel $pp \rightarrow H \rightarrow \gamma\gamma$ with all relevant experimental cuts included. We find that both the reweighted PYTHIA and the reweighted MC@NLO match very well the accepted cross-section as predicted by FEHIP. We next study distributions that have been proposed to discriminate between the Higgs signal and the background. Both R(PYTHIA) and R(MC@NLO) describe the kinematic distributions well. They match the NNLO fixed-order result away from kinematic features, and exhibit the resummation present in the event generators near the kinematic boundaries.

We proceed to study the decay channel $pp \rightarrow H \rightarrow W^+W^- \rightarrow l^+l^-\nu\bar{\nu}$. It is important to understand distributions in this channel at the LHC, since a direct reconstruction of

16

the Higgs boson mass peak is not possible because of the two neutrinos in the final state. We can not yet directly compare lepton distributions with the NNLO result, since FEHIP does not yet contain the decay $H \rightarrow W^+W^- \rightarrow l^+l^-\nu\bar{\nu}$. We study lepton and missing energy distributions using R(PYTHIA), assuming that it predicts the distribution shapes correctly. Since Herwig does not yet contain spin correlations for this channel we do not present results for R(MC@NLO). We find that the reweighting induces very small kinematic shifts. We study the effective K-factor for this channel after all cuts have been applied, and find that it is 10% smaller than the inclusive K-factor. The effect of the rapidity dependence on this effective K-factor is small, about 3%.

In summary, in this paper we study for the first time the detection efficiency for the Higgs boson at the LHC by reweighting parton shower Monte Carlo output to the fully differential Higgs boson cross section at NNLO in QCD. Monte Carlo events from PYTHIA and MC@NLO are normalized to the NNLO calculation of the Higgs boson rapidity and transverse momentum distributions. For Higgs boson events with low $p_\perp$, a constant K-factor is applied, to maintain the resummed shape present in the Monte Carlo simulations. For the $H \rightarrow WW$ channel , where a jet veto is applied, we find a small difference of 3% compared to a similar reweighting approach using only the transverse momentum spectrum. We conclude that the effect of the NNLO Higgs boson rapidity dependence on LHC observables is now accurate to the percent level. The dominant remaining theoretical uncertainties affecting the Higgs boson search at the LHC are: (1) the scale uncertainty arising from truncation of the perturbative expansion at NNLO; (2) the modeling of the low $p_\perp$ Higgs spectrum; (3) the theoretical uncertainties for the backgrounds to the Higgs signal. We believe that the event reweighting studied here is a useful and accurate way of including higher order QCD calculations in Monte-Carlo event generators. It allows us to determine the correct normalization at NNLO after all experimental cuts are included, incorporates the kinematic shifts induced by hard QCD radiation at higher orders, and maintains the resummation present in parton-shower Monte-Carlo programs near kinematic boundaries. We believe that reweighting MC@NLO to match NNLO differential distributions gives a highly accurate description of the Higgs signal at the LHC. We look forward to its application to other processes of phenomenological interest.

[1] ATLAS collaboration, report CERN/LHCC 99-15, ATLAS-TDR-15 vol. 2; CMS collaboration, report CERN/LHCC 97-33, CMS-TDR-4; V. Tisserand, Ph.D. thesis, LAL 97-01, February 1997; M. Wielers, report ATL-PHYS-2002-004; CMS NOTE 2003/033.

[2] V. Buscher and K. Jakobs, Int. J. Mod. Phys. A **20**, 2523 (2005) [arXiv:hep-ph/0504099].

[3] A. Djouadi, arXiv:hep-ph/0503172.

[4] M. Carena and H. E. Haber, Prog. Part. Nucl. Phys. **50**, 63 (2003) [arXiv:hep-ph/0208209].

[5] S. Dawson, Nucl. Phys. **B359**, 283 (1991).

[6] A. Djouadi, M. Spira and P.M. Zerwas, Phys. Lett. **B264**, 440 (1991); D. Graudenz, M. Spira and P.M. Zerwas, Phys. Rev. Lett. **70**, 1372 (1993); M. Spira, A. Djouadi, D. Graudenz and P.M. Zerwas, Nucl. Phys. **B453**, 17 (1995).

[7] R. V. Harlander and W. B. Kilgore, Phys. Rev. Lett. **88**, 201801 (2002) [arXiv:hep-ph/0201206].

[8] C. Anastasiou and K. Melnikov, Nucl. Phys. B **646**, 220 (2002) [arXiv:hep-ph/0207004].

[9] V. Ravindran, J. Smith and W. L. van Neerven, Nucl. Phys. B **665**, 325 (2003) [arXiv:hep-ph/0302135].

[10] S. Moch and A. Vogt, arXiv:hep-ph/0508265.

[11] C. Anastasiou, K. Melnikov and F. Petriello, Phys. Rev. Lett. **93**, 262002 (2004) [arXiv:hep-ph/0409088].

[12] C. Anastasiou, K. Melnikov and F. Petriello, Nucl. Phys. B **724**, 197 (2005) [arXiv:hep-ph/0501130].

[13] C. Balazs and C. P. Yuan, Phys. Lett. B **478**, 192 (2000) [arXiv:hep-ph/0001103];

[14] S. Catani, D. de Florian, M. Grazzini and P. Nason, JHEP **0307**, 028 (2003) [arXiv:hep-ph/0306211].

[15] T. Sjostrand, L. Lonnblad and S. Mrenna, arXiv:hep-ph/0108264.

[16] G. Corcella *et al.*, arXiv:hep-ph/0210213.

[17] S. Frixione and B.R. Webber, JHEP **0206**, 029 (2002);
S. Frixione, P. Nason and B.R. Webber, JHEP **0308**, 007 (2003).

[18] P. Nason, JHEP **0411**, 040 (2004) [arXiv:hep-ph/0409146].

[19] Z. Nagy and D. E. Soper, arXiv:hep-ph/0503053.

[20] M. Kramer, S. Mrenna and D. E. Soper, arXiv:hep-ph/0509127.

[21] G. Davatz, G. Dissertori, M. Dittmar, M. Grazzini and F. Pauss, JHEP **0405**, 009 (2004) [arXiv:hep-ph/0402218].

[22] M. Dittmar and H. K. Dreiner, Phys. Rev. D **55**, 167 (1997) [arXiv:hep-ph/9608317];

[23] S. Catani, D. de Florian and M. Grazzini, JHEP **0201**, 015 (2002).

[24] A. Djouadi, J. Kalinowski and M. Spira, Comput. Phys. Commun. **108**, 56 (1998) [arXiv:hep-ph/9704448].

[25] Z. Bern, L. J. Dixon and C. Schmidt, Phys. Rev. D **66**, 074018 (2002) [arXiv:hep-ph/0206194].

[26] F. Stockli, A. G. Holzner and G. Dissertori, JHEP **0510**, 079 (2005) [arXiv:hep-ph/0509130].

[27] G.Davatz, A.-S. Giolo-Nicollerat, M.Dittmar, CMS-NOTE 2006/047.

[28] G. Bozzi, S. Catani, D. de Florian and M. Grazzini, Phys. Lett. B **564**, 65 (2003) [arXiv:hep-ph/0302104]; G. Bozzi, S. Catani, D. de Florian and M. Grazzini, Nucl. Phys. B **737**, 73 (2006) [arXiv:hep-ph/0508068].